STRUCTURAL EFFICIENCY AND BEHAVIOR OF PRISTINE AND NOTCHED STITCHED STRUCTURE

Dawn C. Jegley
NASA Langley Research Center
Mail stop 190
Hampton VA 23691

ABSTRACT

Two driving factors in aircraft panel design are structural efficiency and response to in-service damage. Stitching through the thickness can improve both of these considerations. Combining stitching with a post-buckling design approach can provide additional improvements. The buckling behavior of stitched structure is considered since lighter structures can be achieved if local skin buckling is allowed to occur at less than design ultimate load. Through-the-thickness stitching can suppress delamination between skin and flange, thereby allowing the structure to reliably carry load into the postbuckling range. Hat-stiffened and rod-stiffened panels in which the skin and flanges were stitched together through-the-thickness prior to curing are considered through experiment and analysis. In both types of panels no mechanical fasteners were used for the assembly. Specimens were loaded to failure in axial compression. In this study all specimens buckled in the skin between the stiffeners and continued to carry load. In addition, the behavior of panels with a severed stringer or notch are considered. Failure loads and strain distributions in the notched panel are compared to those in the unnotched panel.

NOMENCLATURE

A	Planform area (width * frame spacing)
b	Width
DLL	Design Limit Load
DUL	Design Ultimate Load
L	Frame spacing
N_x	Running load at failure (load/width)
N_{xcr}	Running load at buckling (load/width)
W	Panel weight between frames

1. INTRODUCTION

NASA, Boeing and the Air Force Research Laboratory (AFRL) have been involved in the development of technologies needed for future low-cost, light-weight composite structures for transport aircraft for many years. As part of the NASA-Boeing effort, a stitched graphite-epoxy material system was developed with the potential for reducing the weight and cost of transport aircraft load-bearing structure.[1] By stitching through the thickness of a dry graphite-epoxy material system, the labor associated with panel fabrication and assembly can be significantly

reduced. By stitching through the thickness to join elements such as pre-stacked skin segments, stringers, tear straps and frames, the need for mechanical fasteners is almost eliminated. In addition stitching provides a mechanism to reduce damage growth resulting from events such as low-speed impact or discrete-source damage.

Typical design of conventional composite aircraft structure does not allow panels to buckle or existing damage to grow at loads less than Design Ultimate Load (DUL). These restrictions can lead to structures which have much larger failure and buckling loads than the DUL and are, therefore, not structurally efficient. Repeated buckling cycles can lead to delamination between the skin and flange when there is no through the thickness reinforcement, but this delamination problem is eliminated with stitched structure. Therefore, structures that buckle at low loads are no longer automatically deemed unsafe. In addition, stitching has been shown to arrest damage growth and turn cracks in certain circumstances.[1] As a result, a design criterion whereby damage growth from either impact damage or from discrete source damage may be acceptable if it is arrested at a nearby stitch line and the structure, as a whole, can support the load requirement. Allowing limited damage growth from a damage site implies the use of higher strain allowables than would be used if no damage growth were permitted. The use of post-buckled design and higher strain allowables results in a lower weight structure so the structural efficiency is improved compared to structures designed with a no-damage-growth, no-buckling approach.

Structural efficiency is expressed in terms of weight versus load carrying capability.[2,3] Traditionally, the maximum load capacity for a structure was identified as the lowest of the loads corresponding to either allowable stress or strain or the minimum buckling load. For structural panels with adhesively bonded stringers, the primary reason for the buckling restriction is the tendency for bonded stringers to separate from the skin once buckling occurs. If this design restriction can be modified to allow local buckling as long as it doesn't lead to global failure at load less than design ultimate load, more weight- and cost-efficient structures can be realized. Panels can be designed such that the panel is assumed to carry load and remain intact for loads significantly greater than the buckling load.

The goal of this study is to examine the behavior of hat-stiffened and rod-stiffened stitched structures to evaluate the potential weight savings of allowing panels to buckle at load less than ultimate load, as long as the panel does not fail. If the specimen failure load is considered to be the ultimate load, local damage initiation and growth as well as nonlinear post-buckling behavior, must be considered. Analysis and experimentation are used to explore the buckling and post-buckling behavior of stitched composite panels. In addition, the reduction in load carrying capability of notched panels is considered with regard to their bucking and failure loads as compared to unnotched panels. In this study, "hat-stiffened" refers to panels with hat-stiffeners aligned with the loading direction and "rod-stiffened" refers to panels with pultruded carbon rods embedded in the stiffeners in the loading direction. Each test panel was fabricated by the Boeing Company and provided to NASA Langley Research Center for testing.

2. TEST ARTICLES AND ARRANGEMENT

Three specimens, two hat-stiffened and one rod-stiffened, were fabricated from stitched/resin infused graphite-epoxy material. Each panel had stringers aligned with the loading direction and frames perpendicular to the stringers. The hat-stiffened panels were 1.885 m tall, 76.2 cm wide

and contained three hat-stringers and two blade-frames. The hat-stiffener spacing was 25.4 cm and the frame spacing was 61 cm. The rod-stiffened panel was 2.032 m tall, 1.067 m wide and contained seven rod-stringers and four hat-frames. The stringer spacing was 15.24 cm and the frame spacing was 50.8 cm. The geometry of the panels is shown in figure 1. All three panels were fabricated from dry components and then infused using high temperature and vacuum pressure. Skins, flanges and webs were composed of layers of graphite material forms that were prekitted into multi-ply stacks using Hercules, Inc. AS4 fibers. Each nine-ply stack had a $[45/-45/0_2/90/0_2/-45/45]_T$ stacking sequence. Stack thickness was approximately 0.132 cm. Several stacks of the prekitted material are used to build up the desired thickness and configuration. Stringer and frame flanges were stitched to the skin using Vectran fibers and no mechanical fasteners were used for joining. Panels were infused with HexFlow VRM-34 epoxy resin using a (Vacuum Assisted Resin Transfer Molding) VARTM process described in reference 4. In the hat-stiffened panels, the skin and hats were composed of two stacks of material with a total approximate thickness of 0.264 cm. The blade-frames were composed of four stacks with a total approximate thickness of 0.528 cm. The hats and blades were 5.5 and 5.0 cm tall, respectively. Sketches of the cross section of the hat-stiffeners and blade-frames are shown in figures 2a and 2b, respectively. For the rod-stiffened panels, the sides of the hats and the stringer webs were each composed of two stacks with a total approximate thickness of 0.264 cm. Pultruded carbon fiber rods with a diameter of 0.95 cm at the top of the web and a overwrap of one stack were used for the rod-stiffened specimens. The rod-stiffeners were 3.78 cm tall and the frames were 15.2 cm tall. The skin of the rod-stiffened panel was one stack thick. The hat-stringers and hat-frames were supported by Rohacell foam on the inside of the hat. Sketches of the cross section of the rod-stiffeners and hat-frames are shown in figures 3a and 3b, respectively.

Each of the three panels considered in this study had potted loaded ends, metal tubular restraints along the unloaded edges, and a steel support structure attached to each frame at the locations shown in figure 1. The edge and frame restraints and support structure were intended to prevent out-of-plane motion in the form of a single half-wave along the panel length. The edge restraints for the rod-stiffened panel was significantly stiffer than the edge restrain for the hat-stiffened panels, as discussed in reference 5. One hat-stiffened and the rod-stiffened panel were subjected to low speed impact damage to the unstiffened side of the skin prior to loading. Impacts were inflicted using a drop weight impactor with a 2.54-cm diameter tup. Impact locations were mid-length opposite the edge of the flange of the central stiffener. These impacts were intended to represent Barely Visible Impact Damage (BVID) and therefore were to cause no reduction in load-carrying ability. The second hat-stiffened panel was damaged by severing the central stiffener, its flange and the skin underneath it at the mid-length location. The damage was mid-bay to mid-bay or 25.4 cm wide. To ensure the notch did not close completely during the subsequent compressive loading, the notch was wider at the center than at the ends, as shown in figure 4. The damage was meant to represent discrete source damage and would reduce the load carrying capability significantly.

3. INSTRUMENTATION AND PROCEDURE

Each panel was monitored during loading by 20 to 80 strain gages, 8 LVDTs and a full-field optical measurement system. The optical measurement system or Video Image Correlation (VIC)[6] system was used to obtain full field displacement and strain results for the unstiffened side of the skin during the loading of each specimen. The full-field VIC system requires a black

and white speckle pattern be painted on the specimen surface, and uses two cameras positioned at different angles to the specimen surface to simultaneously photograph the specimen at set intervals during the test. In these tests, the specimen was photographed every 2 to 5 seconds, resulting in approximately 150 time steps of data. The VIC system also records the load from the test machine so images can be related to the corresponding load. The VIC system compares the photographic images and produces three-dimensional displacements and strains. For each panel, the section between the centermost frames was monitored using the VIC system. Data from the strain gages and LVDTs were recorded at a rate of two frames per second.

Photographs of a hat-stiffened and a rod-stiffened panel in the test machine are shown in figure 5. The stiffened surface is painted white to improve the video images and was not monitored using VIC since restraints, instrumentation and shadows would limit the clear vision area of a VIC image.

Each panel was loaded in a series of tests at a load rate of between 100,000 and 200,000 N/min. Even though each panel was subjected to BVID prior to loading, these impacts are not visible in the VIC data, and are not considered in the current paper.

4. FINITE ELEMENT ANALYSIS

An analytical evaluation of each panel was conducted using the computer code STAGS.[7] The finite element models for pristine hat-stiffened and rod-stiffened panels are shown in figure 6a and 6b, respectively. Sections of the models showing the severed stiffener region are shown in figure 7. In all cases, the skin, flanges, hats, and frames were represented by quadrilateral shell element. The hat-stiffened panel models included approximately 14,193 shell elements and the rod-stiffened panel models included approximately 80,648 shell elements. The rod-stiffened panel model also includes beam elements representing the rod and overwrap portion of the stiffener and connectors to attach the beams to the shells representing the webs.

The foam inside the hats in all three panels was modeled as part of the shell elements representing the hat tops and webs. This assumption was adequate since the foam carried a negligible amount of load but restrained buckling of the hat webs. For all three panels, the material properties are based on the compression properties for a stack of material,[1] such that the axial stiffness is 63.6 GPa, the lateral stiffness is 32.1 GPa, the shear stiffness is 15.6 GPa, and Poisson's ratio is 0.397. These properties were determined from fabricated stacks, and therefore already take into account the influence of the stitches on the in-plane properties. In addition, the pultruded rods were modeled as beam elements with a stiffness of 124 GPa for both rod-stiffened panels.

The loaded ends of each panel inside the potting were restrained by forcing all lateral and out-of-plane displacements to be zero inside the potted region. The edge restraint system did not fully prevent the unloaded edges of the panel from moving out of plane, as discussed in reference 5. Based on those findings, no edge restraints are included in the present study for the hat-stiffened panels but edge restraints are included for the rod-stiffened panels. Frame supports were included in the analyses of both types of panels by applying displacement at the fixture-frame attachment points representative of the motion determined during the test through full-field displacement measurements. Since the fixture for the rod-stiffened panel provided significantly

more support than the one for the hat-stiffened panel, no displacement at the fixture-frame connection points was permitted in the analysis of the rod-stiffened panels.

Buckling and geometrically nonlinear analysis was conducted for each panel. In the nonlinear analysis, the deformation shape of the buckling mode associated with the minimum local buckling load for each panel was used as a trigger to get past convergence difficulties. The amplitude of the applied deformation was approximately 0.025 cm or approximately 20% of a stack thickness, which would be large enough to overcome numerical difficulties in reaching a converged solution.

5. RESULTS AND DISCUSSION

Experimental results for one impact-damaged hat-stiffened panel, one impact-damaged rod-stiffened panel and one notched hat-stiffened panel are presented. Analytical results for pristine and notched hat-stiffened and rod-stiffened panels are also presented. Since the impact damage was minimal, the impact-damaged panels are assumed to display the same behavior as a pristine panel in the following discussion. Pristine and impact-damaged panels are referred to as unnotched panels herein. Displacements, strains, buckling loads and failure loads are presented for all panels considered. The structural efficiency of these panels is then discussed.

5.1 Panel Behavior

Experimental and analytical results for the total end-shortening and the shortening between the two centermost frames are shown in figures 8 and 9 for hat-stiffened and rod-stiffened panels, respectively. Experimental and analytical results for unnotched panels are shown in blue while results for notched panels are shown in red. Experimental results are represented by solid lines and analytical results are represented by dashed lines. The four curves on the left side of the plot represent the total end shortening while the four curves on the right side of the plot represent the shortening between frames. All shortening results are reasonably linear except near the failure load, indicating that local buckling did not significantly reduce the global panel stiffness. Details of the buckling behavior are described below.

The experimental full-field deformation in the center region between frames for the unnotched hat-stiffened panel is shown in figure 10a for a load level of approximately 640 kN, which is immediately prior to the failure load of 641.7 kN. The unloaded edges of the panel and the frame locations display out-of-plane deformation despite the presence of restraint systems. The influence of the restraint system is discussed in reference 5. Since the edge restraints were not fully effective, they were not included in the analytical model and an applied displacement at the locations where the frame attaches to the support structure was applied such that the maximum deformation of 0.76 cm was applied at a load of 640 kN so that the boundary conditions of the analysis would match the test. The analytical full-field deformation in the center region between frames for the unnotched hat-stiffened panel is shown in figure 10b for a load level of approximately 640 kN. Buckles develop between the stiffeners in the full field data and in the nonlinear analysis at approximately 440 kN of load, resulting in a failure load of approximately 1.44 times the local buckling load.

A similar process of evaluation was completed for the unnotched rod-stiffened panel. The experimental full-field out-of-plane deformations are shown in figure 11a for a load of

approximately 885.1 kN, which is just less than the failure load of 889.6 kN. The unloaded edges of the panel and the frame locations display significantly less out-of-plane deformation for the rod-stiffened panel than for the hat-stiffened panel. For this reason the edge restraints were included in the analytical model of the rod-stiffened panel and displacement at the locations where the frame attached to the support fixture is prevented. The analytical full-field deformation in the center region between frames for the unnotched rod-stiffened panel is shown in figure 11b for a load of approximately loads of 885 kN. The full field displacement data and the nonlinear analysis show buckling between the stiffeners at approximately 356 kN which corresponds to failure at a load 2.48 times the local buckling load.

To further evaluate the buckling and post-bucking behavior, the strains in the skin at the mid-length location mid-bay are shown in figure 12 for the hat-stiffened panels. The axial strain half way between stiffeners for the unnotched panel and 0.63 cm from the notch tip in the notched panel are shown, where blue curves represent the unnotched panel and red curves represent the notched panel. Experimental results are shown as solid lines and analytical results are shown as dashed lines. Back-to-back strain gage locations are shown. The analytical and experimental results agree until failure initiates from the notch tip. At that point, the measured strain becomes somewhat erratic at this location. The compressive strain at 0.63 cm from the tip is approximately 0.0072 cm/cm when the failure initiates, which corresponds to a load of approximately 200 kN. In the experiment, the crack growth arrested at a load of approximately 267 kN. Finite element analysis indicates that the strain in the skin element next to the flange when final failure occurs at 420.8 kN is 0.0059 cm/cm, as shown in figure 13. Note that the failure load of the notched hat stiffened panel with two intact stringers is approximately 66 percent of the failure load of the unnotched panel with three stringers, implying that final failure load is driven by the reduction of cross sectional area available to carry the load rather than a stress concentration at the notch tip or a buckling behavior.

Analysis indicates that for both hat-stiffened and rod-stiffened notched panels the presence of the notch induces out-of-plane deformation in the vicinity of the notch tips and interacts with the local buckling behavior. Since the panels have the same material, stacking sequence and stitch pattern, the behavior at the notch tip of a rod-stiffened panel is assumed to be the same as for a hat-stiffened panel. The axial strain from experiment and analysis mid-bay for the unnotched rod-stiffened panels is shown in figure 14 by blue curves. Experimental results are shown as solid lines and analytical results are shown as dashed lines. The mid-bay location shown for this panel is mid-length between the two bottom-most frames rather than the central frames because that was the location of the strain gages. In addition both gages are on the stiffened side of the panel rather than back-to-back. However, based on the deformation pattern shown in figure 11, and the strain results, these gages are located in different ½ waves, so the surface strains go in opposite directions after buckling. The analytical results for a panel with a mid-length notch of the type applied to the hat panel are shown in figure 14 as red curves with short dashes for strain at a location 0.63 cm from the notch tip. Based on the results from the hat-stiffened notched panel, failure initiation in the rod-stiffened panel is assumed to occur at approximately 0.0072 cm/cm near the notch tip, which corresponds to a load of approximately 422 kN.

If a similar crack arrestment behavior happened in the rod-stiffened panel as in the hat-stiffened panel, arrestment would be expected to occur, followed by a failure at the flange termination location at a strain of approximately of .0059 cm/cm. However a converged solution could not

be achieved with the mid-bay to mid-bay notch with strains away from the notch at that level so elements were removed from the notched rod-stiffened panel model to lengthen the crack to within 0.63 cm of the flanges of the adjacent stiffeners. A failure load was determined based on the assumption that the strain in the element next to the flange of the stiffener adjacent to the severed stiffener reached the same strain as in the hat panel, or 0.0059 cm/cm prior to failure. This assumption lead to a failure in the rod-stiffened panel of approximately 433 kN.

5.2 Structural Efficiency

Structural efficiency is typically expressed in terms of weight versus load carrying capability.[2,3] In the past, these values would be based on global or local buckling with no load carrying capability considered for loads greater than the buckling load. However, since the purpose of this study is to evaluate the potential weight savings of allowing panels to buckle prior to ultimate load, buckling is not considered to be the maximum allowable load. Aerodynamic requirements which could limit the magnitude of buckles for a structure in flight are not considered herein. To eliminate the effects of length, efficiency is expressed herein as weight/(planform area * length) (W/AL) and running load/length (N_x/L), as discussed in reference 2. However, the length used in this study is the length between frames rather than total panel length since most previous studies based their findings on panels without frames. Similarly, only the weight of the panel between frames is considered (i.e. frame weight is not included). Using this format, a lower weight ratio for a given load ratio and conversely, a higher load ratio for a given weight ratio, indicates a more structurally efficient design. The panels considered herein have thin skins and would be appropriate for fuselage structure rather than the more heavily loaded wing structure discussed in references 2 and 3 so the weight parameter for the panels in the current study is less than the panels in those studies. W/AL for both the rod-stiffened and hat-stiffened panels with the geometry described above is 0.00012 kN/cm^3 compared to typical wing panels where W/AL is greater than 0.00019 kN/cm^3.

To be consistent with prior studies, structural efficiency calculations are based on DUL. Based on the results described in the previous section, DUL can be determined by five different assumptions and the structural efficiency can be calculated for each case, as shown figure 15. Structural efficiencies based on the assumption that ultimate load is the failure load (shown as filled blue bars), that the ultimate load is the buckling load (shown as crosshatched blue bars), the load at which damage from the notch begins to grow (shown as filled red bars), the failure of the notched panel is design limit load (shown as pink bars) and where the failure of the notched panel is 70% of design limit load (shown as cross-hatched red bars). The results for the blue bars are based on behavior of an unnotched panel and the results for the red bars are based on a notched panel. DUL is always 1.5 times DLL. DUL would be determined by the lower of one criterion from the notched panel and one criterion from the unnotched panel.

Comparing the blue bars indicates that allowing an unnotched panel to buckle at loads less than DUL can improve structural efficiency by 31 percent in the hat- and 55 percent in the rod-stiffened panel. However, the driving factor in determining DUL is often the behavior in the presence of a notch. The most conservative approach is to define the load at which damage begins to grow from the notch as DLL. DUL is then determined by multiplying this value by 1.5. This assumption reduces DUL by approximately 50 and 30 percent in the hat-stiffened and rod-stiffened panels, respectively, compared to the DUL of the unnotched panels with no

restrictions on buckling. Less conservative approaches are to allow the damage to grow and arrest and to assume that the load at which the panel fails is DLL or that the failure load is 70% DLL. If DLL is the notched panel failure load, the DUL for the hat-stiffened panel is approximately the same as the DUL for the unnotched panel with no restrictions on buckling. If DLL is the notched panel failure load, the DUL for the rod-stiffened panel is approximately 75 percent of the DUL for the unnotched panel with no restrictions on buckling. In both cases, if the failure of the notched panel is assumed to be 70% of DLL, the notched condition is not the most critical condition.

Allowing post-buckling behavior to be considered when determining design loads can significantly increase DUL. Allowing damage arrestment to be considered so that initial damage growth does not indicate final failure results in a more structurally efficient design in both the hat- and rod-stiffened panels.

6. SUMMARY

Experiment and analyses of hat-stiffened and rod-stiffened panels with through-the-thickness stitching was used to evaluate buckling and failure behavior of unnotched panels. Experimentation on a notched hat-stiffened panel was extrapolated to evaluate the behavior of a similar panel with rod-stiffeners instead of hats. In both cases, allowing post-buckling behavior to be considered when determining design loads can significantly increase design ultimate load. Allowing damage arrestment to be considered so that initial damage growth does not indicate final failure can result in a more structurally efficient design in both the hat- and rod-stiffened panels. The hat and rod-stiffened panels were found to have the same weight parameter in a structural efficiency comparison. The rod-stiffened panels were 10 to 20 percent more structurally efficient than the hat-stiffened panels based on several criteria for determining DUL. However, if buckling is not permitted at load less than DUL, the hat-stiffened panel was more efficient that the rod-stiffened panel because of the thicker skin in the hat-stiffened panel. These results indicate that the structural efficiency must be considered on a case-by-case basis to determine the most structurally efficient design.

7. REFERENCES

1. Karal, M., “AST Composite Wing Program - Executive Summary.” NASA CR 2001-210650, August 2001.
2. Williams, J., Anderson, M., Rhodes, M., Starnes, J., & Stroud, J. “Recent Developments in the Design, Testing and Impact-Damage Tolerance of Stiffened Composite Panels.” NASA TM 80077, 1979.
3. Jegley, D., “Study of Compression-Loaded and Impact Damaged Structurally Efficient Graphite-Thermoplastic Trapezoidal-Corrugation Sandwich and Semisandwich Panels.” NASA TP 3264, November 1992.
4. Velicki, A., “Damage Arresting Composites for Shaped Vehicles, Phase I Final Report.” NASA CR-2009-215932, September 2009.
5. Jegley, D., “The Influence of Restraint Systems on Panel Behavior.” presented at the Society of Experimental Mechanics annual meeting, Mohegan Sun, June 2011.

6. McGowan, D., Ambur, D., and McNeil, S., “Full-field Structural Response of Composite Structures: Analysis and Experiment.” presented at the 44th AIAA/ASME/ASCE/AHS Structures, Dynamics and Materials Conference, AIAA 2003-1623, Norfolk, VA, April 2003.
7. Rankin, C., Brogan, F., Loden, W., and Cabiness, H., 2001. "STAGS User Manual, Version 4.0." Lockheed Martin Missiles and Space Company, Incorporated.

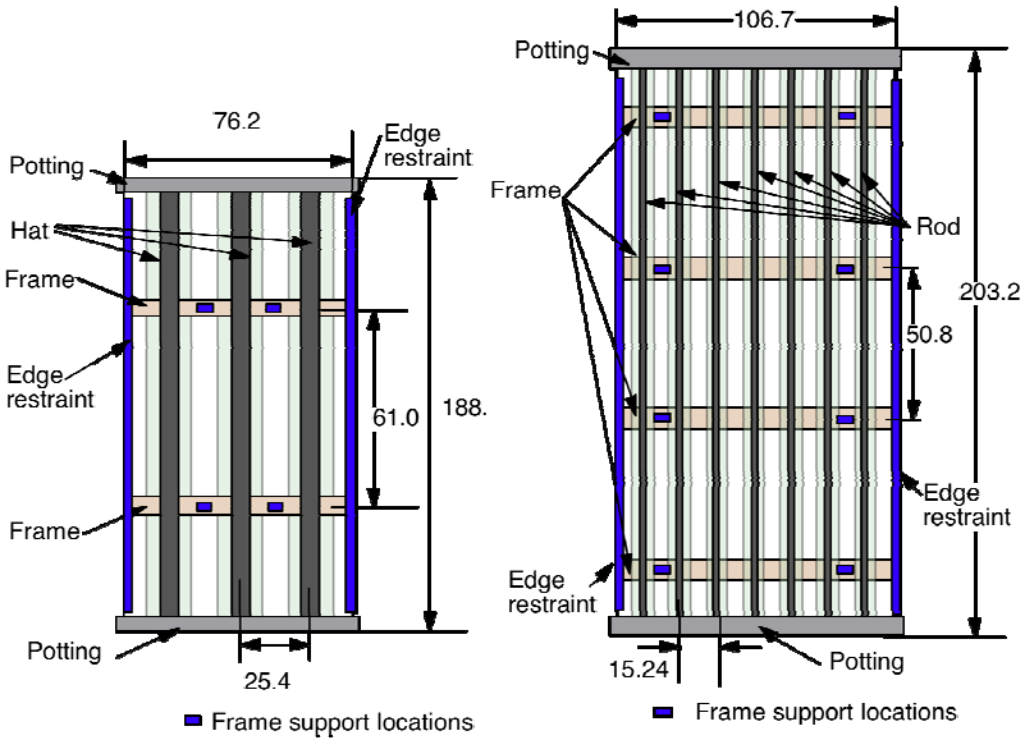

a) Hat-stiffened b) Rod-stiffened

Figure 1. Panel geometry. Dimensions are in cm.

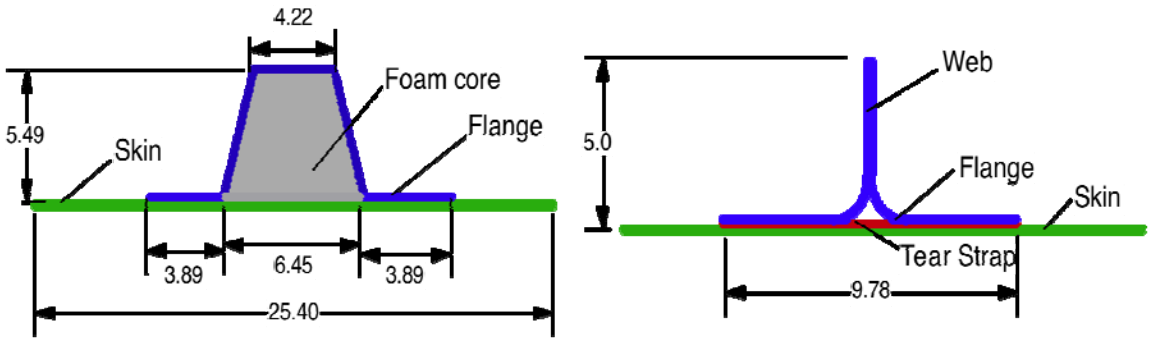

a) Stringer b) Frame

Figure 2. Hat-stiffened panel stiffeners. Dimensions are in cm.

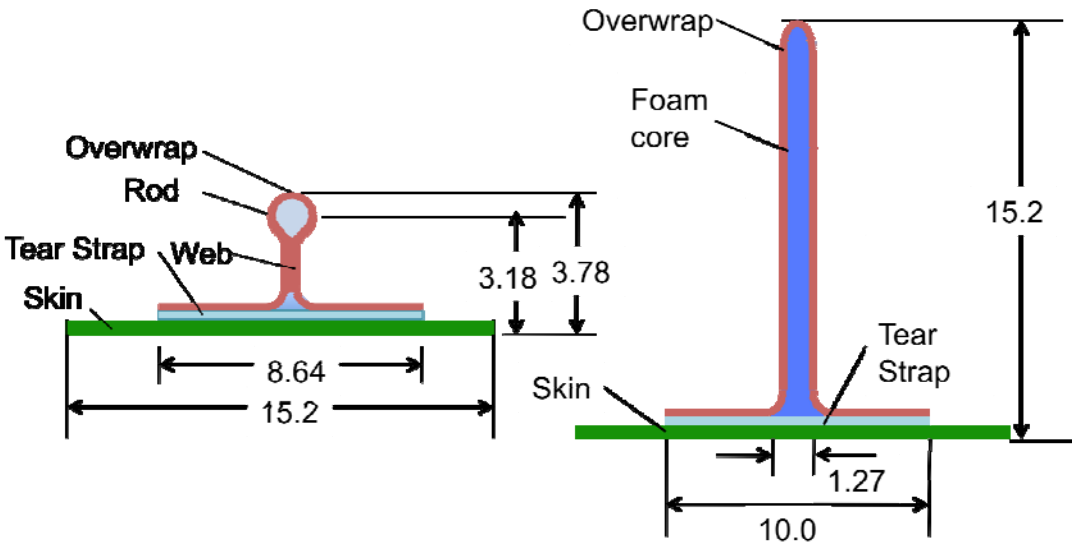

a) Stringer b) Frame

Figure 3. Rod-stiffened panel stiffeners. Dimensions are in cm.

Figure 4. Notch in hat-stiffened panel.

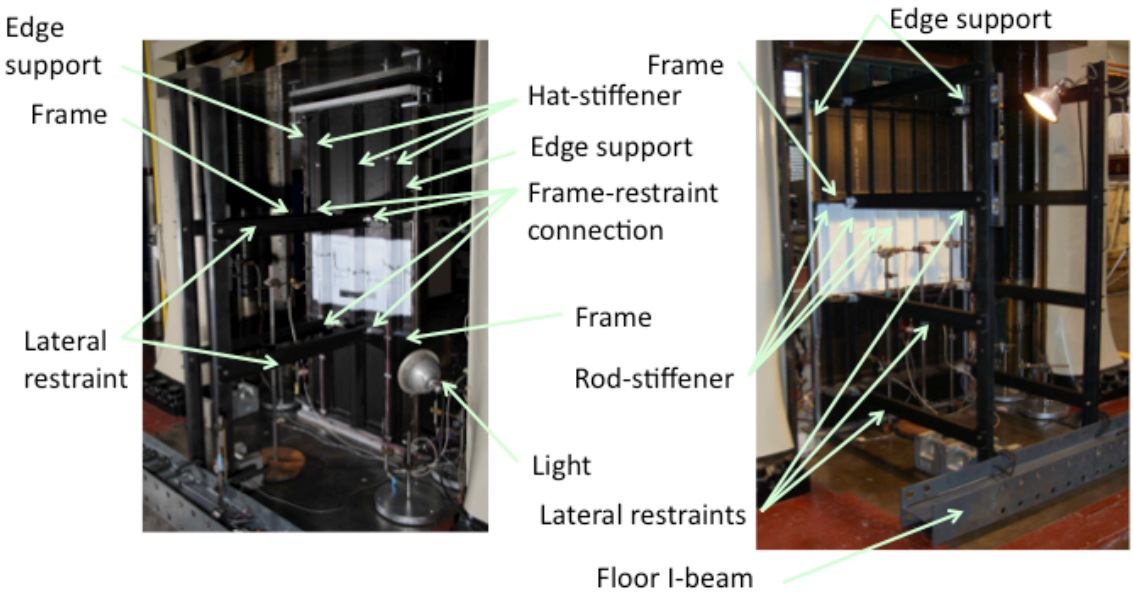

a) Hat-stiffened b) Rod-stiffened

Figure 5. Impact-damaged panels in test machine.

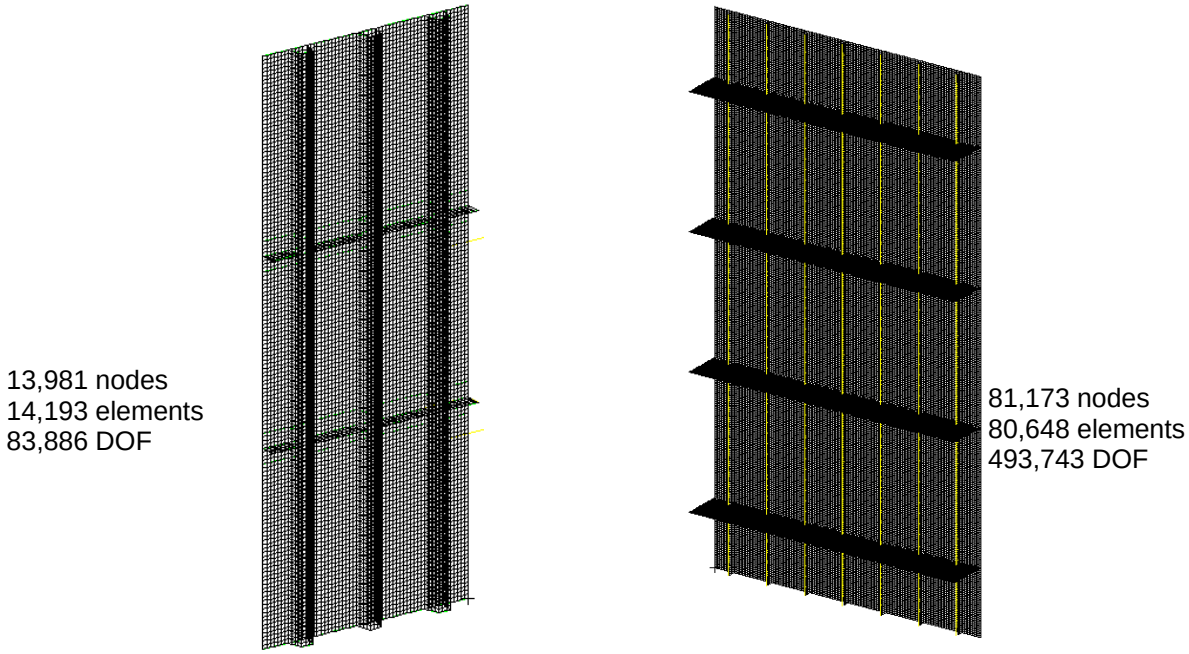

a) Hat-stiffened b) Rod-stiffened

Figure 6. Finite element models.

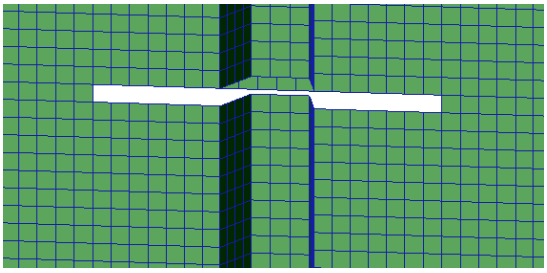

a) Hat-stiffened

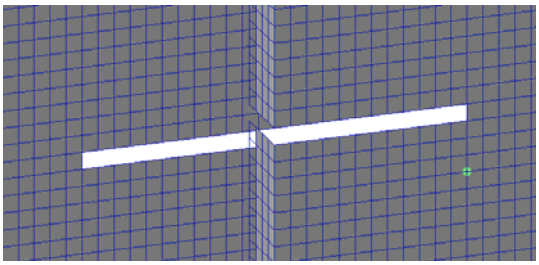

b) Rod-stiffened

Figure 7. Models of notch.

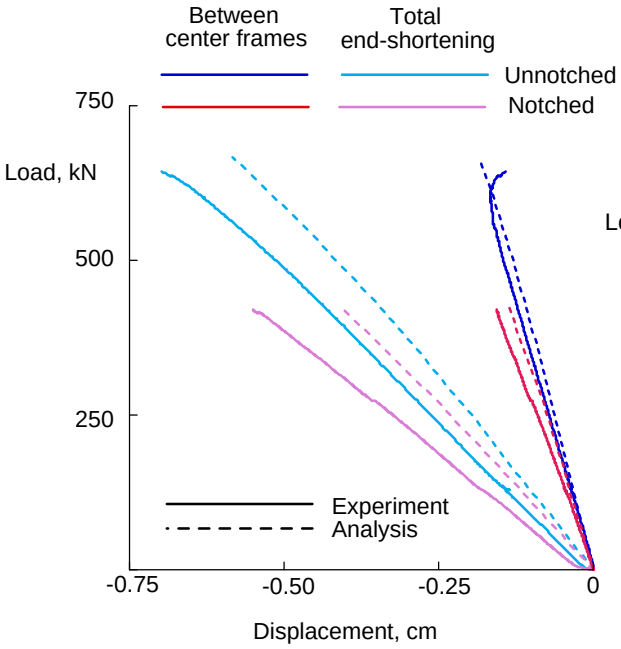

Figure 8. Shortening of hat-stiffened panels.

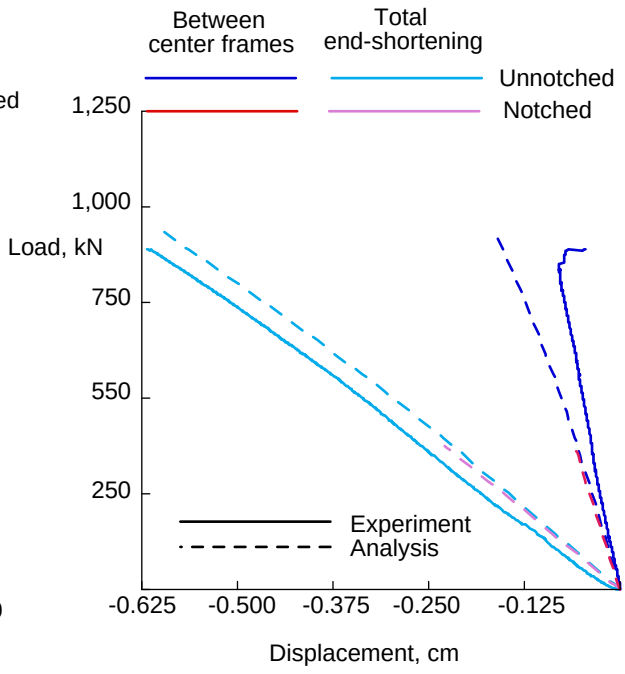

Figure 9. Shortening of rod-stiffened panels.

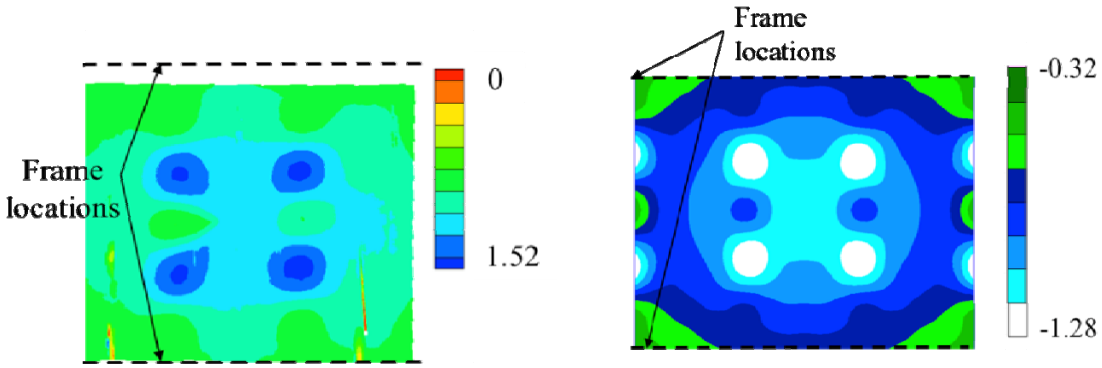

a) Experiment b) Analysis

Figure 10. Full-field out-of-plane deformation in center region of unotched hat-stiffened panel at 99.8% of failure load. Displacements in cm.

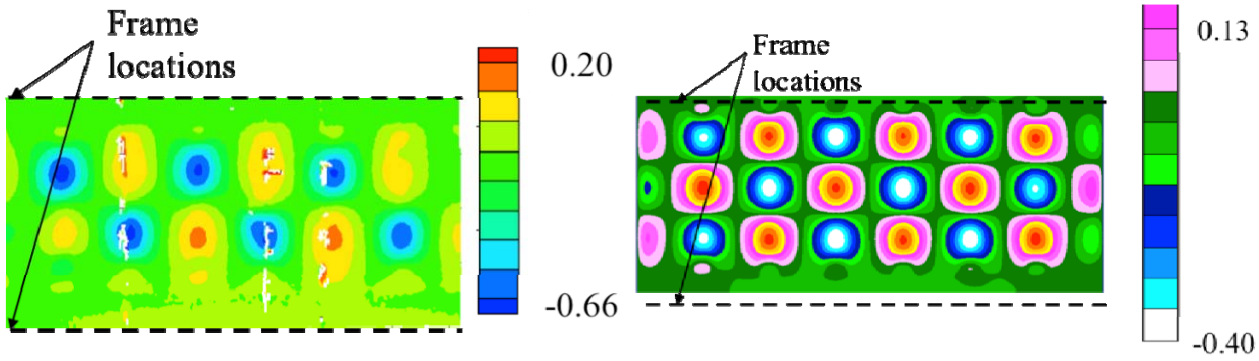

a) Experiment b) Analysis

Figure 11. Full-field out-of-plane deformation in center region of unnotched rod-stiffened panel at 99% of failure load. Displacements in cm.

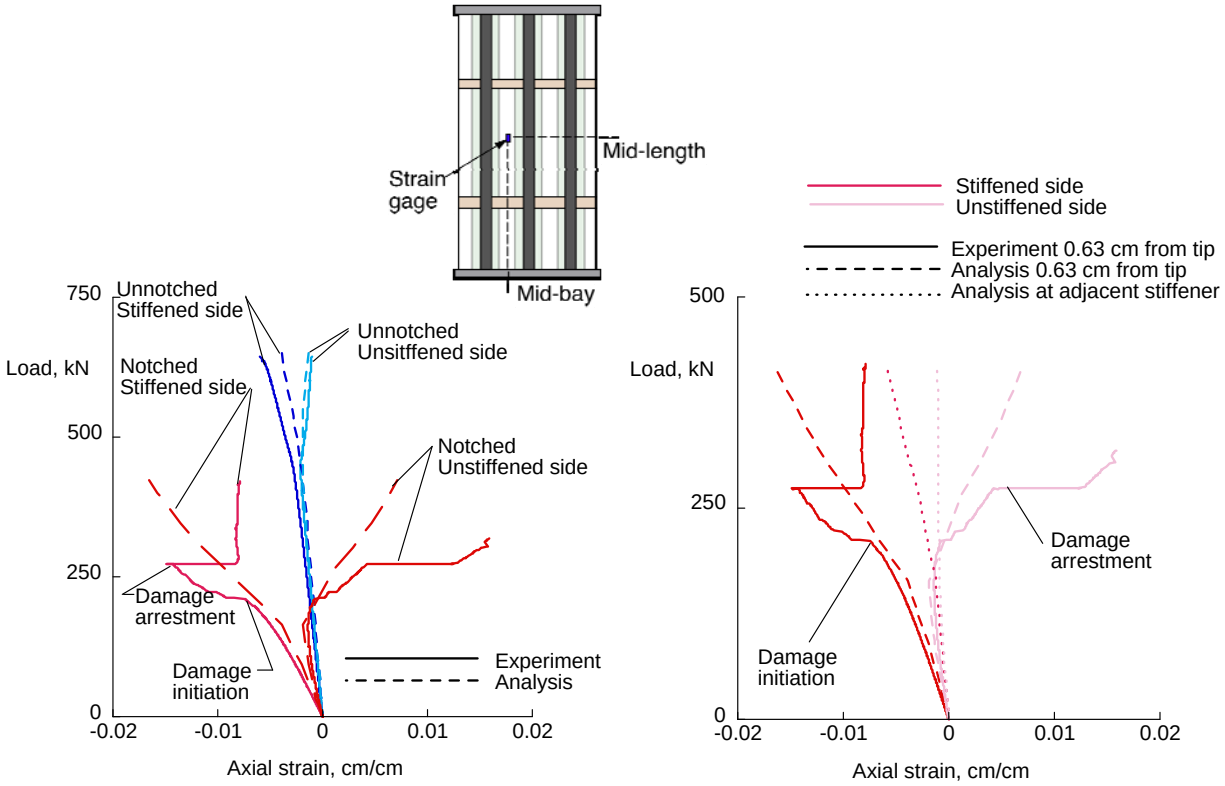

Figure 12. Skin strains in hat-stiffened panels. Figure 13. Notch strains in hat-stiffened panels.

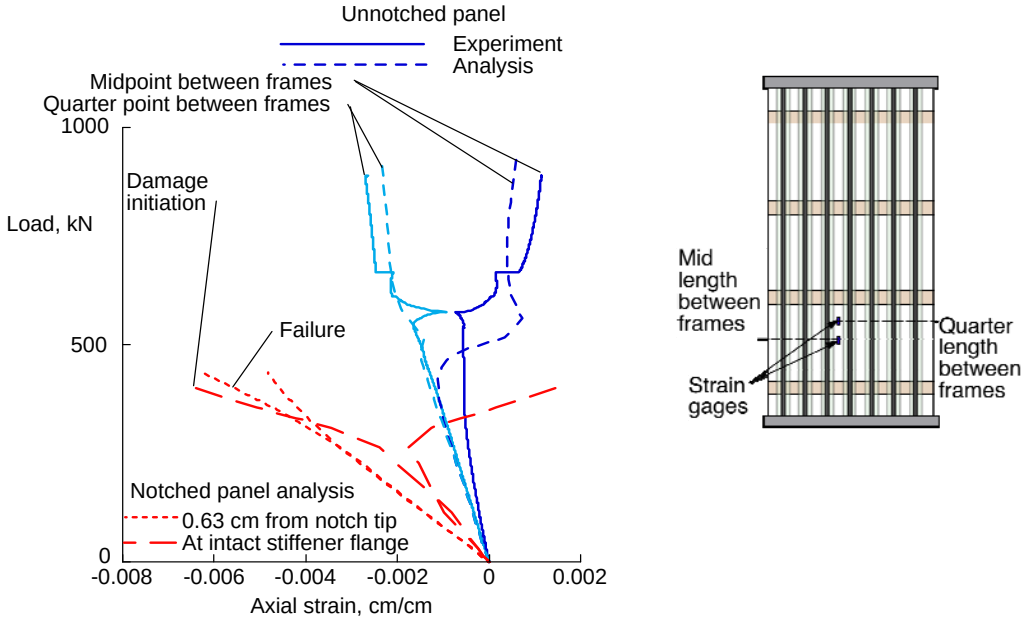

Figure 14. Skin strains in rod-stiffened panels.

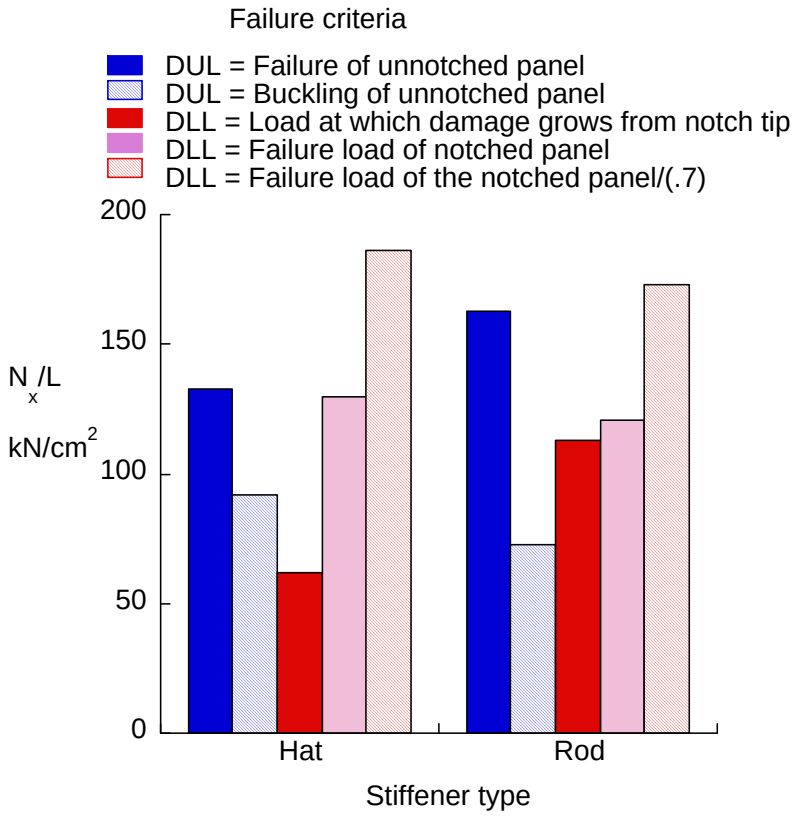

Figure 15. Structural efficiency of hat- and rod-stiffened panels based on Design Ultimate Load.